Research Article Vol. 7, No. 10 / October 2020 / Optica 1409

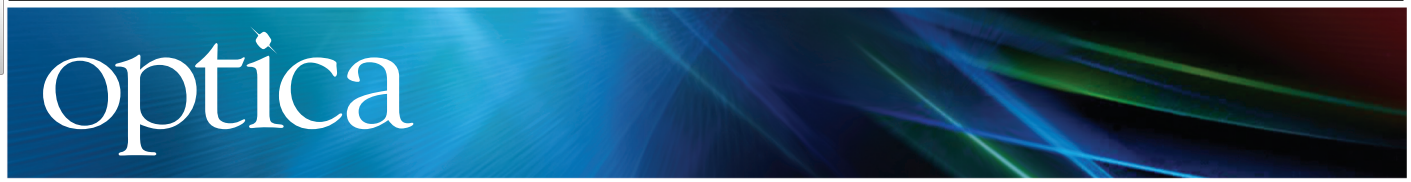

# Monolithic thin-disk laser and amplifier concept

Raoul-Amadeus Lorbeer,* Benjamin Ewers, Christopher Santek, Denise Beisecker, Jochen Speiser, and Thomas Dekorsy

*German Aerospace Center (DLR), Institute of Technical Physics, Pfaffenwaldring 38-40, 70569 Stuttgart, Germany*
**Corresponding author: raoul.lorbeer@dlr.de*

*Received 21 July 2020; revised 21 August 2020; accepted 21 August 2020 (Doc. ID 402164); published 12 October 2020*

**Thin-disk lasers are indispensable in photonics research as well as in a multitude of industrial applications. They represent a unique class of laser and amplifier architecture that provides kW output power with excellent properties concerning beam quality, long-term stability, thermal management, and power scalability. For many applications, a reduced complexity of the laser and its size would be highly beneficial. The necessary multipass transitions in thin-disk lasers and amplifiers typically require sophisticated multi-mirror arrangements. Here, we present a monolithic version of the pump concept for thin-disk lasers and amplifiers, where the thin disk is replaced by a thin, wedged gain medium acting as a wedged optical trap. The wedge is coated in a peculiar manner in order to allow for efficient in- and out-coupling of the pump and laser radiation from the wedge. This concept transfers the complexity of the multi-mirror optics into the thin disk itself in a monolithic fashion. With this concept, we achieved 890 W of CW output power, 59% slope efficiency, optical-to-optical efficiency of 50%, and a gain factor greater than 10 for small signals. This demonstrates that this new concept is capable of reaching the kW power regime with minimum complexity and size.**



https://doi.org/10.1364/OPTICA.402164

## 1. INTRODUCTION

Solid state lasers and amplifiers enable a plethora of applications in basic research and industry. Fiber lasers, slab lasers, and thin-disk lasers exhibit excellent beam quality at kW power levels in CW and pulsed modes [1].

All three concepts achieve efficient thermal management by using a large surface-to-volume ratio. In the case of the thin-disk laser—invented in the 1990s especially to enable high-power operation of ytterbium-doped laser crystals—this is reached by cooling the relatively large (back) surface of the thin disk [2,3]. The cooled surface is coated highly reflective (HR) for the laser wavelength and acts as a resonator mirror, so the cooling will not interfere with the laser, and the main temperature gradients will be parallel to the laser beam. Pump radiation is applied from the front side. This design was quickly transferred to industrial applications: in 1997, Jenoptik produced the first commercial thin-disk laser, a 10 W Nd:YVO system; in 1999, Trumpf presented the first 1 kW thin-disk laser. In the following decades, thin-disk lasers addressed a large range of laser concepts and laser applications for science and industry—from high-power CW operation to sub-ps oscillators and amplifiers [4–6]. Currently, high-power thin-disk lasers with more than 10 kW out of one disk and good beam quality (sufficient for welding applications) are available [7]. One specific benefit of the thin-disk laser is the large gain area—this allows for large beam diameters and low fluences. Working at a low fluence is especially useful for the amplification of short pulses. Additionally, the thin disk combines these low fluences with a small amount of material inside the resonator. This results in low nonlinearities that, e.g., enable chirped pulse amplification (CPA)-free amplification of 750 fs pulses [8]. Many commercial and scientific thin-disk amplifiers are realized as regenerative amplifiers using electro-optical switches. The suitability of the thin disk for high efficiencies at high power also inspired the development of geometrical multipass amplifiers to overcome the power and energy limitations of the electro-optical switches. The comparably low single-pass gain of the thin disk (due to the small thickness) is challenging for multipass amplification, but several concepts were developed, including methods to control the beam quality. One example is the concept described in Ref. [9] that allowed after adaption to larger beam sizes for pulse energies of more than 300 mJ at low repetition rates [10]. A variation of this multipass concept was realized during the last years, achieving more than 1.4 kW with ps pulses and high repetition rate, using 80 passes through the thin disk [11]. For many applications, more compact multipass amplifier arrangements would be beneficial. Additionally, the optical multipass geometry usually necessary for pumping due to the small single-pass absorption of the thin disk also prevents compact solutions.

Here, we demonstrate a new concept for thin-disk lasers and amplifiers that allows reduction of the number of folding optics for pumping and amplification to an absolute minimum.

We introduce a wedge to the thin disk, which breaks its rotational symmetry and introduces a new plane of symmetry. This

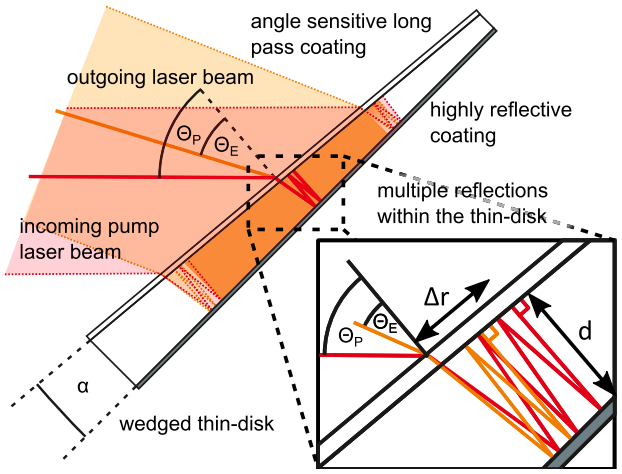


**Fig. 1.** Close-up sketch of wedged thin-disk geometry. Indicated are the wedge angle $\alpha$, the two incidence angles for pump ($\Theta_P$) and lasing ($\Theta_E$) radiation, as well as the local thickness $d$ and beam displacement $\Delta r$. The upper surface is coated as a long pass, while the bottom (back) side is coated with a wide-angle highly reflective coating glued onto a diamond heat sink.

converts the gain medium into a wedged optical trap for the pump light. Optical wedge traps have been investigated as an optimization method for detectors [12,13]. Nevertheless, these trap detectors are illuminated from the edge of the wedge, which is undesirable in the case of a thin-disk laser. For application in a thin-disk laser, it is necessary to introduce a specialized multilayer dielectric coating on top of the wedge. This top coating—as any dielectric coating—exhibits an angle-dependent reflectivity [14] and is designed as a long-pass (LP) filter. The rear side of the thin disk is coated with an HR coating. Due to the wedge, the reflected angle of incidence (AOI) after the reflection is reduced slightly, which suffices to change the reflectivity experienced by the beam at the LP surface significantly. As depicted in Fig. 1, this allows coupling of laser radiation into the wedge trap at any given point on the surface.

With this approach, we demonstrate a CW output power of 890 W, 59% slope efficiency, 50% optical-to-optical efficiency, and a small signal gain factor of 10 in an extremely compact design.

## 2. LASER DESIGN AND CHARACTERIZATION METHODS

### A. Wedged Thin-Disk Properties

The wedge under test was analyzed in great detail in order to understand the dependencies of the relevant parameters. If not stated otherwise, the angles related to laser radiation are given in air. The wedge is designed with a wedge angle of $\alpha = 1°$ starting at a thickness of 100 μm and over a diameter of 15 mm, reaching a thickness of 360 μm. The wedge is made from an 7 at-% Yb:LuAG crystal. The HR coating (NANEO, Germany) is designed to reflect more than 99.99% at 969 nm for an AOI between 0° and 52°, as well as 99.99% at 1030 nm for an AOI between 0° to 38°. Therefore, the coating is HR for all relevant angles and will be treated as a perfect mirror for the following considerations. The angle-dependent front coating is supposed to start transmitting $s$-polarized laser radiation at 1030 nm at 27.5° and unpolarized pump radiation of 969 nm at 45.5° AOI. In blocking regions, the coating is expected to exceed 99% reflectivity while transmitting more than 99% in the passband.

This results in the angle-dependent reflective behavior of the front coating displayed in Fig. 2. The reflection curves in Fig. 2 were measured with unpolarized Fourier-transform infrared (FTIR) spectroscopy. Due to the unpolarized pump radiation, the coating was specifically optimized to have reduced polarization effects. $S$-polarized radiation is expected to experience a slightly steeper LP edge. For details on the procedures and results, see Supplement 1.

The wedged thin disk with these dielectric coatings works as follows: the angle-sensitive LP coating faces the laser and pump radiation, as depicted in Fig. 1. Figure 3 shows the corresponding LP-edge shift depending on the AOI.

The monochromatic laser light is highly reflected at an AOI of 0° to 23°, and at a threshold AOI of 27°, the same wavelength is transmitted (Fig. 2 purple and brown line). Given that the laser radiation is introduced from the thicker end of the wedge, the angle relative to the HR surface introduces a reduction of the AOI below the threshold angle after one reflection, and the laser beam is trapped for multiple reflections (compare Fig. 1) [16,17]. This is also true for the pump radiation indicated in green and red in Fig. 2.

The number $N$ of reflections at the HR coating of the wedge can be estimated by dividing the internal AOI $\Theta_{\text{internal}} = \arcsin(\sin(\Theta)/n)$ by the wedge angle [16]:

$$N \approx \frac{\Theta_{\text{internal}}}{\alpha}, \tag{1}$$

with $n$ as the refractive index within the laser crystal. These values obviously are delicately connected to the actual wedge angle, which we assume to have a tolerance of 0.1°. Therefore, the number of reflections for the seed and pump laser beams may be estimated to $N_{\lambda=969} = 22 \pm 2$ and $N_{\lambda=1030} = 14 \pm 2$, respectively.

The average spatial displacement $\Delta r$ due to the larger AOI and multiple reflections as indicated in Fig. 1 may be estimated with [16]

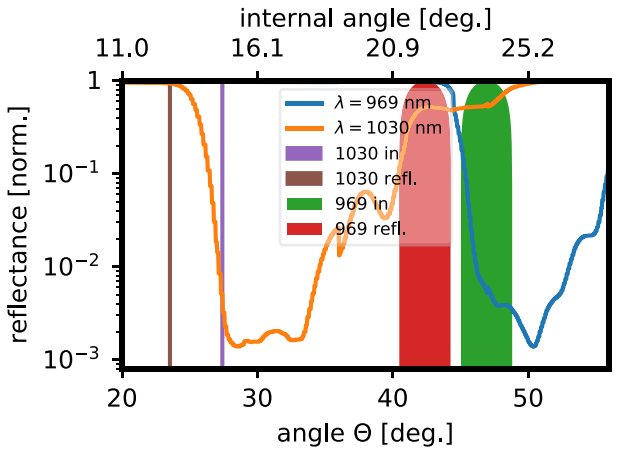


**Fig. 2.** Angle-dependent reconstruction of the reflectivity of the angle-dependent coating at 969 nm (blue) and 1030 nm (orange). Possible pump and lasing radiation angles of incidence are indicated in purple and green, respectively. The widths of the pump bars indicate the angle distribution due to pump brightness limitation. Furthermore, corresponding angles after one reflection are indicated in brown and red. The reflection curves were measured with FTIR spectroscopy. For details on the procedures and results, see Supplement 1.

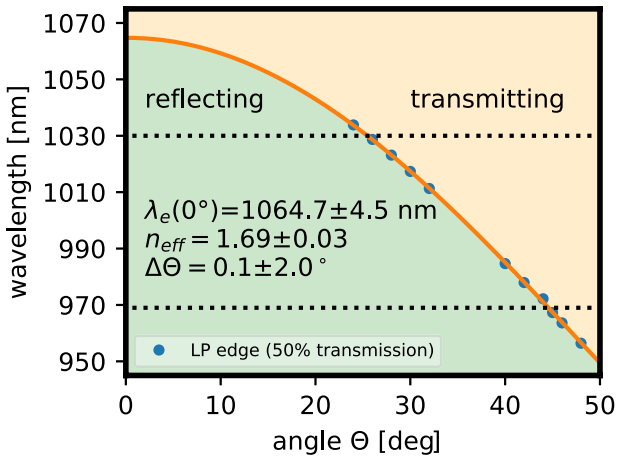


**Fig. 3.** Dependency of the spectral position of the filter edge on the angle of incidence [15] as measured (circles) with fitted model (orange line). With $\lambda_e(0°)$ as edge position at 0° AOI, $n_{\text{eff}}$ es effective refractive index of the coating and $\Delta\Theta$ as a correction for a potential offset angle during the measurement. Reflecting (green) and transmitting (orange) regions are indicated as filled areas. For details on the procedures and results, see Supplement 1.

$$\Delta r \approx -\frac{\ln|\cos(\Theta_{\text{internal}})|}{\Theta_{\text{internal}}} N\langle d\rangle, \tag{2}$$

with $\langle d\rangle$ as the average wedge thickness experienced by the beam. This results in $\Delta r_{\lambda=969} \approx 4.5\langle d\rangle$ and $\Delta r_{\lambda=1030} \approx 1.8\langle d\rangle$.

### B. Lasing Setup and Rigrod Analysis

In order to demonstrate the new concept and verify the kW scalability, a simple multimode I-resonator was chosen. This resonator is established with concave output couplers of 1 m radius of curvature (custom coatings, Laseroptik, Germany) and the thin-disk wedge at an incidence angle optimized for the lasing wavelength of 1030 nm. The basic setup is displayed in Fig. 4.

By changing the output coupler, different output coupling ratios were evaluated. As the pump source, a 969 nm fiber coupled laser diode array was chosen (IS57.1, DILAS, Germany). The system is wavelength stabilized and allows optical pumping with up to 2 kW via a 1 mm, NA 0.2 high-power fiber system. The fiber output was re-imaged via a cooled collimation lens ($f = 50$ mm) and a mirror (BB1-E03, Thorlabs, USA) onto the wedged thin disk with an approximate AOI of 45°. The pump spot reached

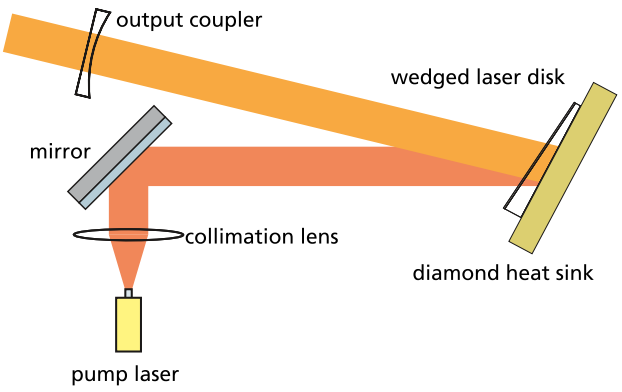


**Fig. 4.** Optical setup of monolithic pump geometry placed in an I-resonator.

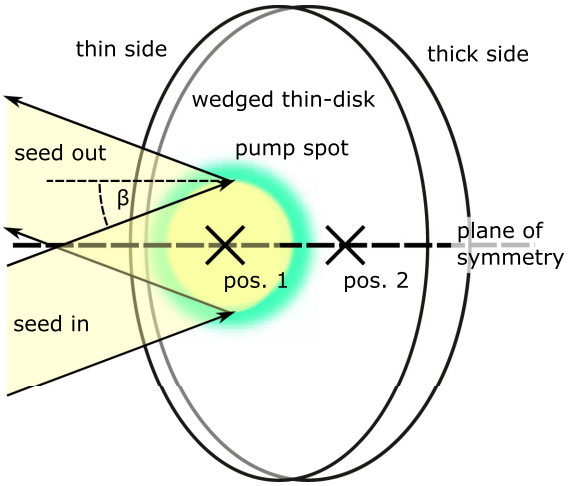


**Fig. 5.** Arrangement for small signal gain measurement. Indicated are the plane of symmetry of the wedged thin disk, the pump spot, and the included angle of incidence $\beta$ between the seed beam and the plane of symmetry. Test positions pos.1 and pos. 2 are indicated.

a diameter of 6 mm. It was placed at position 1 on the wedge, as indicated in Fig. 5. This placement did yield slightly better results in our pre-tests. The wedged thin disk itself is glued onto a diamond heat sink and cooled with a 13°C water jet directed at the back side of the heat sink. Input pump powers were measured with a power meter (L1500W, Ophir Optronics, Israel) after the collimation lens and fitted to the laser diode current for reference in lasing experiments. Lasing powers were measured directly after the output coupler via one steering mirror (BB1-E03, Thorlabs, USA) and one concave lens ($f = -30$ mm, Thorlabs, USA) onto the power meter (L1500W, Ophir Optronics, Israel). Temperatures were determined contactless with a thermal camera (Seek Shot, Seek Thermal, USA).

The Rigrod analysis is an established method for determination of laser efficiency. Slope efficiencies $\eta_{\text{slope}}$ for the I-resonator were evaluated for different transmission values of the concave out-coupling mirrors.

The Rigrod model as described in Ref. [18] is given in Eq. (3):

$$\eta_L = \frac{P_{\text{out}}}{P_{\text{avail}}} = \frac{T}{(1+\sqrt{R_1/R_2})(1-\sqrt{R_1 R_2})}\left[1+\frac{1}{2}\frac{\ln(R_1 R_2)}{\ln G_0}\right], \tag{3}$$

with $R_1 = 1 - T$ and $R_2 = 1 - L$. The remaining fitting parameters are internal losses $L$ and single-pass small signal gain $G_0$.

The transmission $T$ of the output coupler was determined by reference laser transmission measurements at 1030 nm.

To utilize the well-determinable slope efficiencies instead of the available lasing power $P_{\text{avail}}$, which is not available from measurements, we did alter Eq. (3) slightly.

For moderate degrees of output coupling and output powers well above the lasing threshold, the relation between output power $P_{\text{out}}$ and pump power $P_{\text{pump}}$ may be approximated by

$$P_{\text{out}} \approx \eta_{\text{slope}} \cdot P_{\text{Pump}}, \tag{4}$$

which for full equality results in the relationship

$$\eta_{\text{slope}} = \eta_L \frac{P_{\text{avail}}}{P_{\text{Pump}}} = \eta_L \cdot \eta_{\text{in}}. \tag{5}$$

Since $\eta_L$ as well as $\eta_{\text{slope}}$ are constants, $\eta_{\text{in}}$ must be constant, too.

Introducing Eq. (5) into Eq. (3) then results in the measurable relation

$$\eta_{\text{slope}} = \frac{T \cdot \eta_{\text{in}}}{(1+\sqrt{R_1/R_2})(1-\sqrt{R_1 R_2})}\left[1+\frac{1}{2}\frac{\ln(R_1 R_2)}{\ln G_0}\right], \quad (6)$$

where $\eta_{\text{in}}$ is introduced as a new fit parameter. Equation (6) unfortunately, due to the approximation in Eq. (4), is not suitable to determine $G_0$ any longer. Therefore, emphasis will be on the results concerning the loss $L$ of the system.

### C. Small Signal Gain of Wedged Thin Disk

The small signal gain of the wedged thin disk was determined in the setup depicted in Fig. 5. By introducing an additional angle $\beta$ relative to the plane of mirror symmetry of the wedge, the returning light may be separated from the incoming seed laser light. The seed laser beam was extended to 6 mm in diameter to match the diameter of the pump spot. The incident ($P_{\text{in}}$) and emitted ($P_{\text{out}}$) radiation powers were measured with the same power meter (PD300-3 W, Ophir Optronics, Israel); background fluorescence ($P_{\text{fluo}}$) was measured separately and subtracted before calculating the gain factor $G$ of the emitted over the incident radiation power:

$$G = \frac{P_{\text{out}} - P_{\text{fluo}}}{P_{\text{in}}}. \quad (7)$$

The seed laser (Matchbox 1030-15B, Integrated Optics, Lithuania) produced 1030 nm CW emission at approx. 160 mW. The amplification factor with respect to the pump power was determined for a pump spot on two positions, as indicated in Fig. 5. Position 1 is 5 mm apart from the thin edge with thickness $d \approx 190$ µm, and position 2 is 5 mm apart from the thick edge with thickness $d \approx 270$ µm. Furthermore, the seed laser was attenuated to 9.6 mW and 3.2 mW for comparison.

## 3. RESULTS

### A. Lasing Test and Rigrod Analysis

In the high-power lasing test, the system reached 890 W of output power (Fig. 6). At output powers below 700 W, it appears feasible to achieve 1 kW of output power with 2 kW of pump power. Nevertheless, saturation effects are observed above 700 W of output power, currently limiting the system to 890 W. During the test, temperatures of up to 130°C were reached. High temperatures are known to have a fundamental influence on the efficiency of quasi-three-level laser materials such as Yb:YAG [3] due to the thermal population of the lower laser level. Gain and absorption coefficients are reduced at higher temperatures [19].

Since the core temperature of the thin-disk wedge is not accessible, a contactless thermal camera was chosen to document surface temperature of the wedge. To generate plausible readings, the $\epsilon$ setting for the thermal camera was chosen as 0.8. With pump radiation turned off, this gave a reading of 13°C, as determined by the known coolant temperature.

The slope efficiency reaches $59 \pm 3\%$, while the optical-to-optical efficiency of the system peaks at $50 \pm 3\%$. These results were achieved with a concave output coupler ($R = 1$ m) and a transmission of 36%.

Multiple measurements of the optical-to-optical properties of the I-resonator setup have been performed to deduce system losses and optical-to-optical efficiency. By changing the output transmission, different slope efficiencies were determined and used to evaluate the fitting parameters of the adapted Rigrod model in Eq. (6). The fit result is shown in Fig. 7 and suggests internal losses of $4.1 \pm 0.7\%$ and a maximum achievable system slope efficiency of $70 \pm 5\%$ if no internal losses were present.

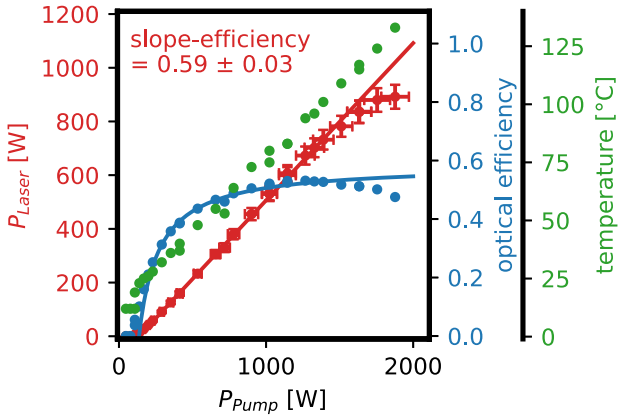


**Fig. 6.** Multimode high-power test. Displayed are input pump power $P_{\text{Pump}}$, output lasing power $P_{\text{Laser}}$, optical-to-optical efficiency, and wedge temperature.

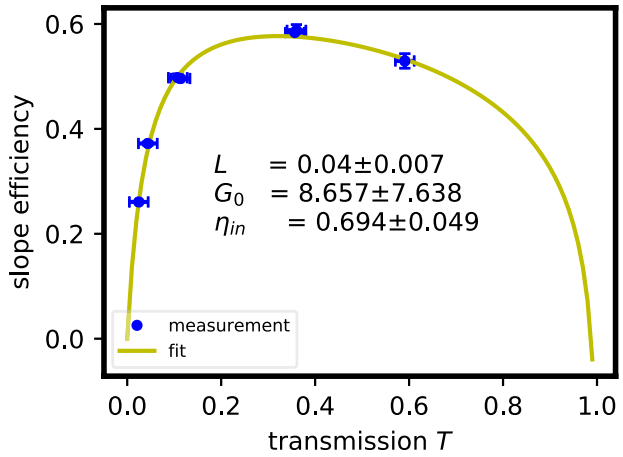


**Fig. 7.** Adapted Rigrod plot with fitting parameters $L$, $G_0$, and $\eta_{\text{in}}$. The loss determined is approximately 4%.

### B. Small Signal Gain of Wedged Thin Disk

The amplification factor with respect to the pump power for a pump spot on position 1 and on position 2 is shown in Fig. 8.

A variation of the seed power by one order of magnitude results in similar gain values; this indicates that the results represent small signal gain. Without pump radiation, the wedge absorbs the seed radiation as described by the Beer–Lambert law. This relation allows testing the consistency between absorption and design geometry. The transmission of the non-pumped wedge is 0.47 at position 1 and 0.33 at position 2 for the 1030 nm seed laser. The ratio of optical extinction from both positions can be calculated from the measurements to be $\ln(0.47)/\ln(0.33) = 1.46$. Assuming the design edge thickness of 100 µm increasing to 360 µm over 15 mm and an adjustment of the pump spot centers shifted 5 mm ± 1 mm

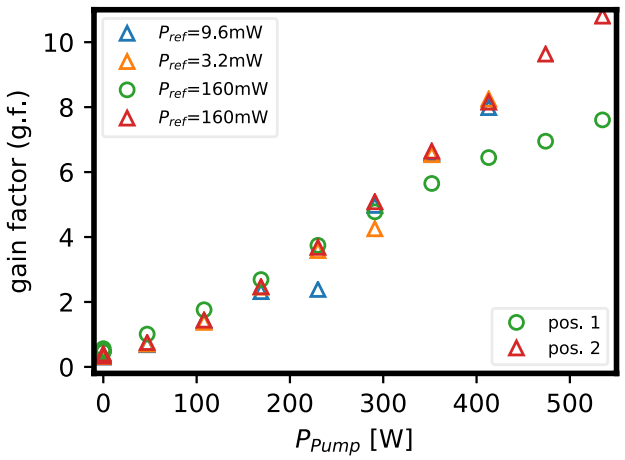


**Fig. 8.** Small signal gain at multiple seed powers and wedge positions 1 (circles) and 2 (triangles). Position 1 is centered 5 mm away from the thin edge, and position 2 is centered 5 mm from the thick edge (compare Fig. 5).

from the wedge borders also results in a thickness ratio of 187 μm ± 20 μm/273 μm ± 20 μm = 1.46 ± 0.2. The slope of the small signal gain factor increases in a similar manner. Linear fitting of the measurements with 160 mW seed power results in a ratio of $0.021\frac{g.f.}{W}/0.015\frac{g.f.}{W} = 1.40$. The increase can be interpreted only as a tendency since multiple effects have an influence on this parameter.

## 4. DISCUSSION

In the design phase of the experiment losses induced by the coating posted a major concern.

As discussed in Supplement 1, the spectral properties of the coating allow utilization of a total of 95% of the pump radiation. A direct measurement of the first surface reflected pump light results in 7% losses, which indicates that the divergence angle of the pump light is still larger as expected. Furthermore, it may be deduced that increasing the spot size would also reduce the divergence of the pump beam and therefore increase pump efficiency even further. A similar evaluation for the lasing wavelength results in a loss of 4.6% per round trip. Direct measurement yields reflective losses between 1.7% and 4.4%. The adapted Rigrod analysis suggests a loss of 4.1 ± 0.7%.

As can be seen in Fig. 2, the introduction of the monolithic design introduces beneficial internal angles in the high refractive index laser crystal. As indicated by Eq. (2), reducing the internal AOI and minimizing the wedge thickness also reduces shifting of the multiple reflected echoes and results in a sharp contrast pump spot compared to previous experiments [17] (compare Supplement 1, Fig. S5). Furthermore, this allows for a steeper separating LP edge compared to an LP–air interface at the same wedge angle. A smaller wedge angle leads to moderate thickness changes over the pump spot. With an LP–air interface, the wedge angle would need to be larger, and the thickness would vary significantly more.

To improve pump efficiency without changing the properties of the coating, it might be beneficial to introduce an asymmetric pump light source that has a reduced divergence angle in one direction. This is a typical property of laser diodes; therefore a direct attachment of the pump laser diodes in contrast to a delivery by fiber optics could improve the overall design. This could be improved even further by reimplementing the polarization-dependent properties of the front coating, which were minimized in the current design for the sake of compatibility to the available pump sources.

The monolithic thin-disk wedge approach is strongly dependent on the manufacturing capabilities for wedged thin laser amplifying media such as, e.g., Yb:YAG crystals as well as high-contrast angle-dependent and polarization-independent LP filters. All components are obliged to handle high pump radiation and laser radiation intensities. At this point, we can confirm that pump powers of 2 kW and internal resonator powers of approximately 3 kW are possible with the coatings deposited directly onto the laser crystal. Nevertheless, this does not allow a prediction for the use in pulsed operation yet, which will be the focus of future studies. The bandwidth implications of the demonstrated technology, which become relevant for ultra-short pulses of less than a few ps, are discussed in Supplement 1.

Remaining questions are the slope efficiency of the system, which did not reach literature standards of 80% [20], as well as optimization of the overall beam quality. The asymmetry of the wedge potentially leads to effects such as, e.g., astigmatism. Nevertheless, the monolithic nature of the system should allow for almost static compensations to restore beam quality. Further questions concern the ultimate power limitations, utilization in succeeding amplification stages or in parallel amplifiers, optimum AOIs, and variation of the coating as well as the crystal material itself.

## 5. CONCLUSION

In this paper, we were able to demonstrate that current manufacturing technologies are suitable to achieve all necessary prerequisites to reach 890 W of output power with the wedge disk concept. Due to the complex reflectivity nature of the wedge, reflective losses on the order of 4% are introduced into the system.

Multiple reflections within the wedge increase the amplification per pass, allowing for an output coupler transmission of 36%, strongly compensating for the internal losses.

We believe that improvements based on optimization of a variety of parameters in geometry, material properties, coating properties, and design will allow reducing the losses. Small signal gain was measured to reach an amplification factor of up to 10, and total optical-to-optical efficiency of 50% and slope efficiency of 59% in a multimode I-resonator were demonstrated.

**Acknowledgment.** We want to thank Samantha Siegert for proofreading the paper.

**Disclosures.** R.-A. L., T. D.: German Aerospace Center (DLR), Institute of Technical Physics, WO/2017/194489 (P).

See Supplement 1 for supporting content.

## REFERENCES

1. W. F. Krupke, "Ytterbium solid-state lasers. The first decade," IEEE J. Sel. Top. Quantum Electron. **6**, 1287–1296 (2000).

2. A. Giesen, H. Hügel, A. Voss, K. Wittig, U. Brauch, and H. Opower, "Scalable concept for diode-pumped high-power solid-state lasers," Appl. Phys. B **58**, 365–372 (1994).
3. K. Contag, M. Karszewski, C. Stewen, A. Giesen, and H. Hugel, "Theoretical modelling and experimental investigations of the diode-pumped thin-disk Yb:YAG laser," Quantum Electron. **29**, 697–703 (1999).
4. A. Giesen and J. Speiser, "Fifteen years of work on thin-disk lasers: results and scaling laws," IEEE J. Sel. Top. Quantum Electron. **13**, 598–609 (2007).
5. C. J. Saraceno, F. Emaury, O. H. Heckl, C. R. Baer, M. Hoffmann, C. Schriber, M. Golling, T. Südmeyer, and U. Keller, "275 W average output power from a femtosecond thin disk oscillator operated in a vacuum environment," Opt. Express **20**, 23535–23541 (2012).
6. T. Dietz, M. Jenne, D. Bauer, M. Scharun, D. Sutter, and A. Killi, "Ultrafast thin-disk multi-pass amplifier system providing 1.9 kW of average output power and pulse energies in the 10 mJ range at 1 ps of pulse duration for glass-cleaving applications," Opt. Express **28**, 11415–11423 (2020).
7. S. Feuchtenbeiner, S. Zaske, S.-S. Schad, T. Gottwald, V. Kuhn, S. Kumkar, B. Metzger, A. Killi, P. Haug, and N. Speker, "New generation of compact high power disk lasers," Proc. SPIE **10511**, 105110L (2018).
8. A. Beyertt, D. Müller, D. Nickel, and A. Giesen, "CPA-free femtosecond thin disk Yb:KYW regenerative amplifier with high repetition rate," in *Advanced Solid-State Photonics (TOPS)* (Optical Society of America, 2004), p. 231.
9. A. Antognini, K. Schuhmann, F. D. Amaro, F. Biraben, A. Dax, A. Giesen, T. Graf, T. W. Haensch, P. Indelicato, L. Julien, C.-Y. Kao, P. E. Knowles, F. Kottmann, E. Le Bigot, Y.-W. Liu, L. Ludhova, N. Moschuering, F. Mulhauser, T. Nebel, F. Nez, P. Rabinowitz, C. Schwob, D. Taqqu, and R. Pohl, "Thin-disk Yb:YAG oscillator-amplifier laser, ASE, and effective Yb:YAG lifetime," IEEE J. Quantum Electron. **45**, 993–995 (2009).
10. J. Tümmler, R. Jung, H. Stiel, P. V. Nickles, and W. Sandner, "High-repetition-rate chirped-pulse-amplification thin-disk laser system with joule-level pulse energy," Opt. Lett. **34**, 1378–1380 (2009).
11. J.-P. Negel, A. Loescher, A. Voss, D. Bauer, D. Sutter, A. Killi, M. A. Ahmed, and T. Graf, "Ultrafast thin-disk multipass laser amplifier delivering 1.4 kW (4.7 mJ, 1030 nm) average power converted to 820 W at 515 nm and 234 W at 343 nm," Opt. Express **23**, 21064–21077 (2015).
12. J. H. Lehman, "Pyroelectric trap detector for spectral responsivity measurements," Appl. Opt. **36**, 9117–9118 (1997).
13. S. Woods, J. Proctor, T. Jung, A. Carter, J. Neira, and D. Defibaugh, "Wideband infrared trap detector based upon doped silicon photocurrent devices," Appl. Opt. **57**, D82–D89 (2018).
14. C. R. Pidgeon and S. D. Smith, "Resolving power of multilayer filters in nonparallel light," J. Opt. Soc. Am. **54**, 1459–1466 (1964).
15. M. Lequime, "Tunable thin film filters: review and perspectives," Proc. SPIE **5250**, 302–311 (2004).
16. B. Ewers and R.-A. Lorbeer, "Interference filter based beam confinement for increased mechanical phase modulation," OSA Contin. **2**, 1502–1509 (2019).
17. B. Ewers, R.-A. Lorbeer, A. Fischer, and J. Speiser, "New compact pump geometry for thin disk lasers with a tilted optical long-pass filter," Proc. SPIE **10896**, 108960V (2019).
18. A. E. Siegmann, *Lasers* (University Science Books, 1986).
19. J. Koerner, C. Vorholt, H. Liebetrau, M. Kahle, D. Kloepfel, R. Seifert, J. Hein, and M. C. Kaluza, "Measurement of temperature-dependent absorption and emission spectra of Yb:YAG, Yb:LuAG, and Yb:$CaF_2$ between 20° C and 200° C and predictions on their influence on laser performance," J. Opt. Soc. Am. B **29**, 2493–2502 (2012).
20. B. Weichelt, A. Voss, M. A. Ahmed, and T. Graf, "Enhanced performance of thin-disk lasers by pumping into the zero-phonon line," Opt. Lett. **37**, 3045–3047 (2012).